Applied Energy 329 (2023) 120237

Contents lists available at ScienceDirect

Applied Energy

journal homepage: www.elsevier.com/locate/apenergy

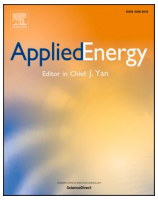

Global sensitivity analysis and optimal design of heat recovery ventilation for zero emission buildings

Peng Liu [a,*], Maria Justo Alonso [a], Hans Martin Mathisen [b]

[a] Department of Architecture, Materials and Structures, SINTEF Community, Trondheim, Norway
[b] Department of Energy and Process Engineering, Norwegian University of Science and Technology, Trondheim, Norway

HIGHLIGHTS

- New insight into annual performance and net energy savings of heat wheel in demand-controlled ventilation.
- The first study to quantify the most influential design parameters of heat recovery and their interaction effects using GSA.
- The optimal design of rotary heat recovery maximises the annual net energy saving amount in heat recovery ventilation.
- The methods and findings contribute to highly energy-efficient ventilation and hence zero emission buildings.

ARTICLE INFO

Keywords:
Energy-efficient ventilation
Rotary heat exchanger
Global sensitivity analysis
Optimal design

ABSTRACT

Energy-efficient building services are necessary to realise zero-emission buildings while maintaining adequate indoor environmental quality. As the share of ventilation heating needs grow in well-insulated and airtight buildings, heat recovery in mechanical ventilation systems is increasingly common. Ventilation heat recovery is one of the most efficient and viable means to reduce ventilation heat losses and save energy. Highly efficient heat exchangers are being developed or applied to maximise the energy-saving potential of heat recovery ventilation. Nevertheless, the effects of practical operating conditions and the constraints of heat recovery – such as variations in ventilation rates, frost protection, and the prevention of an overheated air supply over a long-term period, which may significantly influence realistic recovery rates – have been less considered in efforts to maximise the energy savings. It is unclear which design parameters for heat recovery devices have the greatest effect on the annual energy savings from ventilation.

This study proposes annual efficiency and annual net energy saving models for heat recovery ventilation that consider ventilation rate variations, the longitudinal heat conduction effect and operating controls. We use a global sensitivity analysis to quantify the contributions of various design input parameters to the variation in annual recovery efficiency and annual net energy savings. We identify the most influential parameters and their significant interaction effects for the annual energy performance of heat recovery ventilation. More attention should be paid to these most influential parameters during the design process. Furthermore, the optimal designs for rotary heat exchangers (as identified by a pattern-search optimisation algorithm) can improve annual net energy savings in demand-controlled ventilation by 33–48%, depending on the building areas. In combination with the reference year analysis presented in this study, heat recovery and demand-controlled ventilation can help to meet the need for highly efficient ventilation systems and zero-emission buildings.

1. Introduction

Buildings have been progressively air tightened and insulated to comply with increasingly stringent building energy performance requirements. Heating, ventilation and air conditioning (HVAC) systems, which are vital to sustaining adequate thermal comfort and indoor air quality, potentially account for 30–40 % of the overall energy consumption and about 40–60 % of the total electricity in buildings [1–4]. It is essential to achieve energy-efficient HVAC systems in order to realise zero-energy and zero-emission buildings. In buildings with high levels of thermal insulation, ventilation losses can account for more than 50 % of

* Corresponding author.
E-mail address: peng.liu@sintef.no (P. Liu).

https://doi.org/10.1016/j.apenergy.2022.120237
Received 9 June 2022; Received in revised form 6 October 2022; Accepted 25 October 2022
Available online 10 November 2022

Nomenclature

Parameters

A	Heat transfer area [m^2]
A_k	Cross-sectional area of the matrix wall [m^2]
f	Friction factor [-]
Q	Energy [J]
C^*	Ratio of minimum to maximum heat capacity rates [-]
C_{min}	Minimum heat capacity rate, m^*c_p [W/K]
C_r^*	Ratio of total matrix heat capacity rate
D_h	Hydraulic diameter of flow passages [m]
G	Fluid mass velocity based on the minimum free area [kg/m^2]
g_c	Proportionality constant [-]
t	Temperature [°C]
Eff_i	Hourly temperature efficiency [-]
Eff_{mean}	Operational annual average efficiency [-]
Nu	Nusselt number [-]
c_p	Specific heat of air [J/kg • K]
h	Convective heat transfer coefficient [W/m^2 K]
k	Thermal conductivity [W/(m • K)]
L	Depth of the wheel [m]
m	Mass flow rate [kg/s]
N	Rotation speed [RPM] or hour numbers
Re	Reynolds number [m^2]
U	Overall heat transfer coefficient [W/m^2 K]
X	Input variable
Y	Function value
V_{X_i}	Variance of argument taken over X_i
$E_{X_{\sim i}}$	Mathematical expectation of argument taken over all factors but X_i
S	Sensitivity index
V	Volumetric flow rate [m^3/h]

Subscript

m	Matrix
min	Minimum
w	Wall
T	Total
i	Index

Abbreviations

CAV	Constant air volume
DCV	Demand-controlled ventilation
LHC	Longitudinal heat conduction
NTU	Number of heat transfer units
GSA	Global sensitivity analysis
FP	Factors prioritisation

Greek letters

α	Aspect ratio of the channel
λ	Dimensionless parameter for longitudinal heat conduction
δ	Thickness of the wall [m]
ε	Temperature efficiency
Δp	Pressure drop [Pa]
Φ	Dimensionless parameter
η	Fan efficiency
τ	Time [hour]

total energy loss [5] if no heat recovery is used. Heat recovery systems have been shown to reduce the need for ventilation energy by 80–90 % [6,7]. Consequently, energy-efficient ventilation systems with heat recovery are particularly relevant for highly efficient buildings in cold climates [7].

Some European countries, particularly those with cold weather, implement regulations that mandate energy-efficient ventilation systems that incorporate heat recovery for newly constructed buildings [8]. For example, the Norwegian building regulation TEK 17 [9] for residential buildings requires heat recovery with a temperature efficiency higher than 80 % to meet its energy efficiency target.

Rotary heat exchangers (also known as heat wheels), flat plate heat

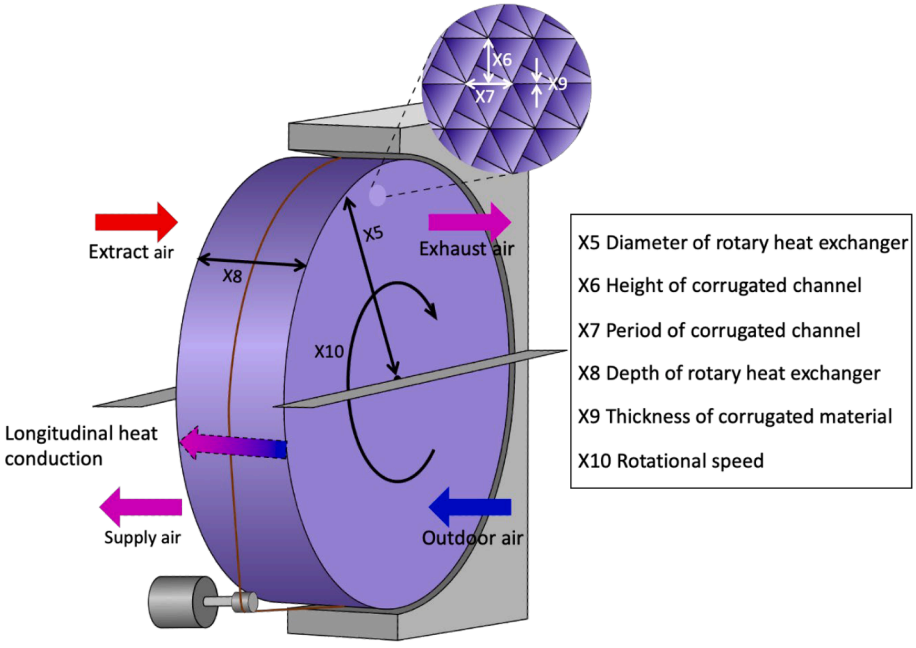

Fig. 1. A rotary heat exchanger in ventilation and its design parameters (the numbering of design parameters X_i is in accordance with the other sections of this study).

exchangers and run-around heat exchangers are commonly used in residential ventilation. Aluminium rotary heat exchangers have been widely utilised in Nordic countries due to their high efficiency and frost tolerance. Fig. 1 shows the working principle of the rotary heat exchanger. In cold climates, sensible heat is recovered by storing heat from the extract air to the rotating matrix. The stored heat is released from the matrix as it rotates to the supply air. In these exchangers, a temperature gradient exists in the aluminium matrix as heat transfer occurs. This causes heat conduction from the hotter to the colder ends of the aluminium matrix, reducing the mean outlet temperature of the supply air in winter conditions. Consequently, the longitudinal heat conduction (LHC) in the metallic matrix along the flow direction can lead to an efficiency reduction of 20 % (from 90 % to 70 %) or more [10,11]. The effects of LHC have often been overlooked in the design and operation of heat recovery units [12,13]. However, recent research has shown that LHC is significant and cannot be neglected, especially for lower airflow rates than the design value [10,12].

DCV is an energy-efficient measure that can reduce ventilation energy use by 30–60 % compared to CAV [14–16]. In principle, the combined use of DCV and heat recovery in ventilation further reduces energy use, and thus contributes to achieving zero-emission buildings with extraordinarily energy-efficient ventilation. DCV often operates at lower airflow rates than the maximum design value. One might expect that in any heat recovery system, reducing airflow rates would always increase temperature efficiency. However, as mentioned above, the presence of higher LHC at lower airflow rates can lead to unexpected reductions in efficiency [17,18]. Therefore, the inefficiency of rotary heat exchangers due to LHC at low airflow rates may reduce or even eliminate the energy-saving benefits of using heat recovery in DCV.

To the authors' knowledge, no studies have examined rotary heat exchangers' annual performance while considering LHC's role in DCV. Moreover, few studies have focused on optimum designs to maximise the nominal temperature efficiency of heat recovery systems at specific conditions, such as the rated condition [19,20]. Nevertheless, heat recovery seldom operates at the nominal condition, as the airflow rates may constantly change in DCV and the efficiency must be regulated according to different operating conditions, as illustrated in Fig. 1.

In cold outdoor conditions, frost forms and accumulates when a heat exchanger's surface temperature falls below the dew point and freezing point in extract air. Frost accumulation on heat exchangers is one of the most frequently reported problems when heat recovery ventilation is applied in cold climates [21]. Accordingly, temperature efficiency is usually reduced to decrease heat exchange and prevent frost [7]. In mild outdoor conditions, the temperature efficiency of heat recovery may need to be reduced to avoid overheating the ventilation air over the supply air temperature setpoint. Most studies aim to improve the momentary temperature efficiency of rotary heat exchangers at the dry and wet testing conditions prescribed in standards such as EN308 [22], and EN13141-1 [23]. The temperature efficiency of rotary heat exchangers depends on the ventilation rate, which is controlled by indoor temperature, CO_2 or other parameters. Temperature efficiency over a design reference year considering airflow rate variations would more accurately reflect the realistic performance of a heat recovery system. Currently, there is no representative function to relate the efficiency of the rotary heat exchanger to the outdoor air temperature and indoor control indicators. Furthermore, the influence of different design parameters of rotary heat exchangers on annual temperature efficiency and annual net energy savings remains unknown.

To maximise the benefit of heat recovery systems, one must take the power consumption of the fans into account. In some cases, fan power consumption can result in very low or not guaranteed energy savings from heat recovery systems. For example, Roulet et al. [24] measured 13 ventilation systems in Switzerland and found that energy savings were small or even negative in several cases. Therefore, the annual net energy savings, which are represented by recovered energy subtracted from the additional fan power, should be maximised to obtain the largest realistic benefit from heat recovery systems and DCV. Nevertheless, few studies have addressed the problem of optimising heat exchangers to maximise annual net energy savings.

This study was carried out to explore the most influential design parameters and identify the optimal design for the annual performance of rotary heat exchangers in DCV. The key contributions and novelty of this work are as follows.

- This study provides new insights into the influence of operating conditions on the annual performance of heat recovery devices. These influence factors include variations in airflow, frost and overheating prevention and LHC in rotary heat exchangers.
- For the first time, the outcome of employing heat recovery considering the contradictory LHC effect is explored for DCV during a design reference year.
- This is the first study to use a variance-based global sensitivity analysis to quantify the most influential design parameters and their interaction effects for rotary heat exchangers in terms of annual recovery efficiency and annual net energy savings.
- A pattern-search optimisation method is used to find the optimal design of rotary heat exchangers that maximises the annual net energy savings.
- The findings should make an important contribution to energy-efficient ventilation and zero-emission buildings.

2. Methods

Fig. 2 illustrates the structured methods applied in this study. The momentary temperature efficiency considering the LHC effect, as well as the pressure drop calculation through rotary heat exchangers and their associated influential design parameters, are first presented in Section 2.1. Sections 2.1 and 2.2 introduce the annual performance of the rotary heat exchanger incorporating different ventilation strategies and operating conditions during a design reference year. In Section 2.3, the design input parameters that affect the annual performance of rotary recovery efficiency are explored using the global sensitivity analysis (GSA) method. Finally, the optimal design of rotary heat exchangers for maximising annual net energy savings in heat recovery ventilation is demonstrated in Section 2.4.

2.1. Mathematical models for temperature efficiency and pressure drop

The momentary temperature efficiency of a rotary heat exchanger is considered the exchanger's key performance indicator. Analytical, numerical and empirical methods that aim to improve the design to obtain a higher temperature efficiency have been developed both with and without considering the LHC effect [11]. This study uses empirical correlations considering the LHC effect to determine rotary heat exchangers' temperature efficiency. The essential equation is built on an extension of the 'effectiveness-NTU' method used to calculate temperature efficiency and is given in Eq. (1). The detailed development of the mathematical equations can be found in [11].

$$\varepsilon = \frac{NTU}{1+NTU}\left[1-\frac{1}{9\left(C_r^*\right)^{1.93}}\right]\left(1-\frac{C_\lambda}{2-C^*}\right) \tag{1}$$

In this study, we consider only balanced airflow rates for rotary heat exchangers. It can be seen from Eq.(1) that the determination of temperature efficiency consists of three parts. The first, $\frac{NTU}{1+NTU}$, accounts for the counterflow recuperator effectiveness. The second, $\left[1-\frac{1}{9\left(C_r^*\right)^{1.93}}\right]$, reflects the influence of the rotation and heat capacity of the exchanger. The last, $\left(1-\frac{C_\lambda}{2-C^*}\right)$, accounts for the impact of LHC. The input parameters of these three parts can be further categorised into parameters that designers can control, operating parameters and other constant parameters (Fig. 3). A summary of the equations to determine the parameters

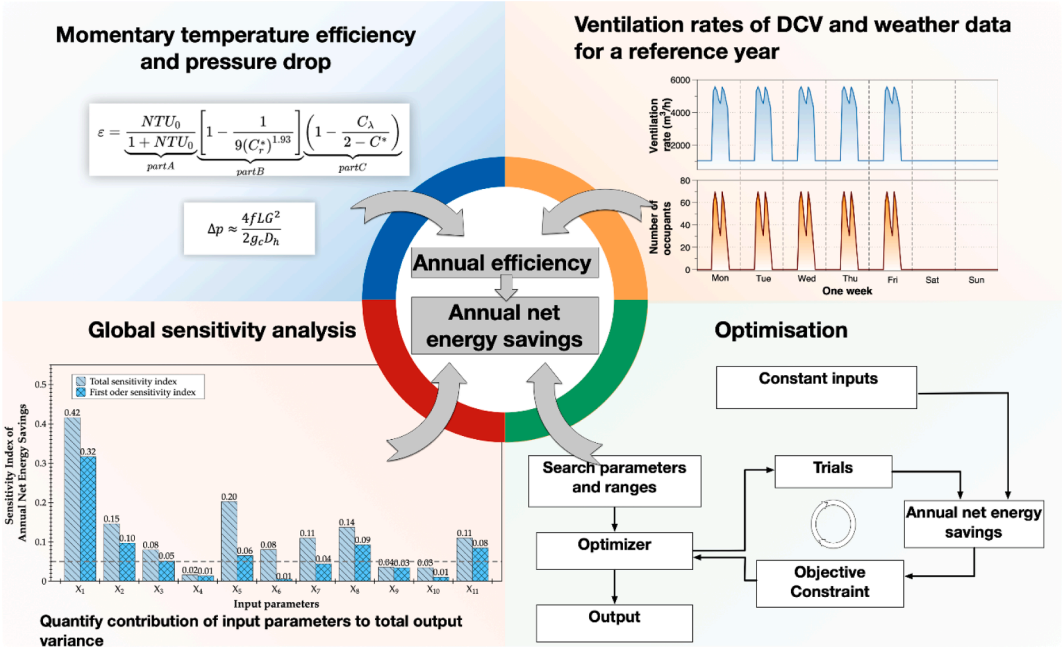

Fig. 2. Illustration of the structured methods used in this study.

in Eq. (1) is presented in Eqs. (2)–(8) below. More detailed definitions and determinations of all the factors in Eq. (1) can be found in [11].

C_λ in Eq. (1) can be calculated as follows:

$$C_\lambda = \frac{1}{1+NTU_o(1+\lambda\Phi)/(1+\lambda NTU_o)} - \frac{1}{1+NTU_o} \tag{2}$$

where Φ denotes a function relationship as in Eq.(3).

$$\Phi \approx \left(\frac{\lambda NTU_o}{1+\lambda NTU_o}\right)^{1/2} tanh\left\{\frac{NTU_O}{[\lambda NTU_o/(1+\lambda NTU_o)]^{1/2}}\right\} \tag{3}$$

λ refers to the ratio of the longitudinal heat conduction, along with the flow direction per unit length, to the heat capacity of the fluid per unit temperature difference. It is defined as

$$\lambda = \frac{k_m A_k}{LC_{min}} \tag{4}$$

λ ranges from 0 to 1. The greater the value of λ, the higher the heat conduction and efficiency loss in the rotary heat exchanger. Eq. (4) shows that good thermal conductors (high k_m) and low airflow rates (C_{min}) yield high LHC and high efficiency loss.

NTU_o is the number of transfer units:

$$NTU_o = \frac{U_o A}{(\dot{m}Cp)_{min}} \tag{5}$$

The overall heat transfer coefficient U_o is

$$U_o = \left(\frac{2}{h} + \frac{\delta}{3k_m}\right)^{-1} \tag{6}$$

$\frac{2}{h}$ represents the convective resistance for the balanced supply and extraction airflows, and $\frac{\delta}{3k_m}$ represents the transverse heat conduction in a rotary heat exchanger [11]. The convective heat transfer coefficient, h, is calculated as

$$h = \frac{Nuk_{air}}{D_h} \tag{7}$$

Nu is determined using the thermal boundary of the constant heat transfer rate for aluminium, a highly conductive material for the matrix, in rotary heat exchangers. The Nusselt number, Nu, is calculated for sinusoidal channels with a laminar flow as follows:

$$Nu_{H1} = 1.9030\left(1+0.4556\alpha+1.2111\alpha^2-1.6805\alpha^3+0.7724\alpha^4-0.1228\alpha^5\right) \tag{8}$$

where α is the aspect ratio (i.e. the ratio of the channel height to the period).

In this work, we examine the commonly used aluminium rotary heat exchanger with sinusoidal corrugations. The operational parameters of rotary heat exchangers are ventilation airflow rates and rotational speed. Ventilation airflow rates vary between different ventilation strategies and with the environmental control indicators such as CO_2, indoor air temperature and the number of occupants. The rotational speed regulates the temperature efficiency of the rotary heat exchangers to prevent the overheating of the supply air and to protect the exchanger from frost. In this article, we employ sensitivity analysis to investigate the influence of the supply air temperature setpoint and the frost protection temperature on the annual average temperature efficiency and energy use for heating the ventilation air.

The hourly temperature efficiency of a rotary heat exchanger is expressed as a function of the outdoor air temperature, as shown in Eq. (9). This equation considers the supply air temperature setpoint, frost protection and overheating prevention for balanced airflow rates in supply and exhaust sides.

$$\mathrm{Eff}_i = \begin{cases} \dfrac{t_{\text{supply}} - t_{\text{outdoor},i}}{t_{\text{indoor},i} - t_{\text{outdoor},i}}, \text{if } \left(t_{\text{outdoor},i} + \varepsilon\left(t_{\text{indoor},i} - t_{\text{outdoor},i}\right) > t_{\text{supply}} > t_{\text{outdoor},i}\right) \\ 0, \text{ if } \left(t_{\text{outdoor},i} > t_{\text{supply}}\right) \\ \dfrac{t_{\text{indoor},i} - t_{\text{frost protection}}}{t_{\text{indoor},i} - t_{\text{outdoor},i}}, \text{ if } \left(t_{\text{indoor},i} - \varepsilon\left(t_{\text{indoor},i} - t_{\text{outdoor},i}\right) < t_{\text{frost protection}}\right) \\ \varepsilon, \text{ (for the rest of conditions)} \end{cases} \tag{9}$$

The first expression in Eq. (9) calculates the temperature efficiency for the case when the maximum temperature supply is limited by overheating prevention (to prevent the temperature of supply air after the heat exchanger from exceeding the supply air setpoint). The second expression ($\mathrm{Eff_i} = 0$) in Eq. (9) represents the case when the heat exchanger is stopped if the outdoor air temperature is higher than the supply air temperature setpoint. Finally, the third expression calculates

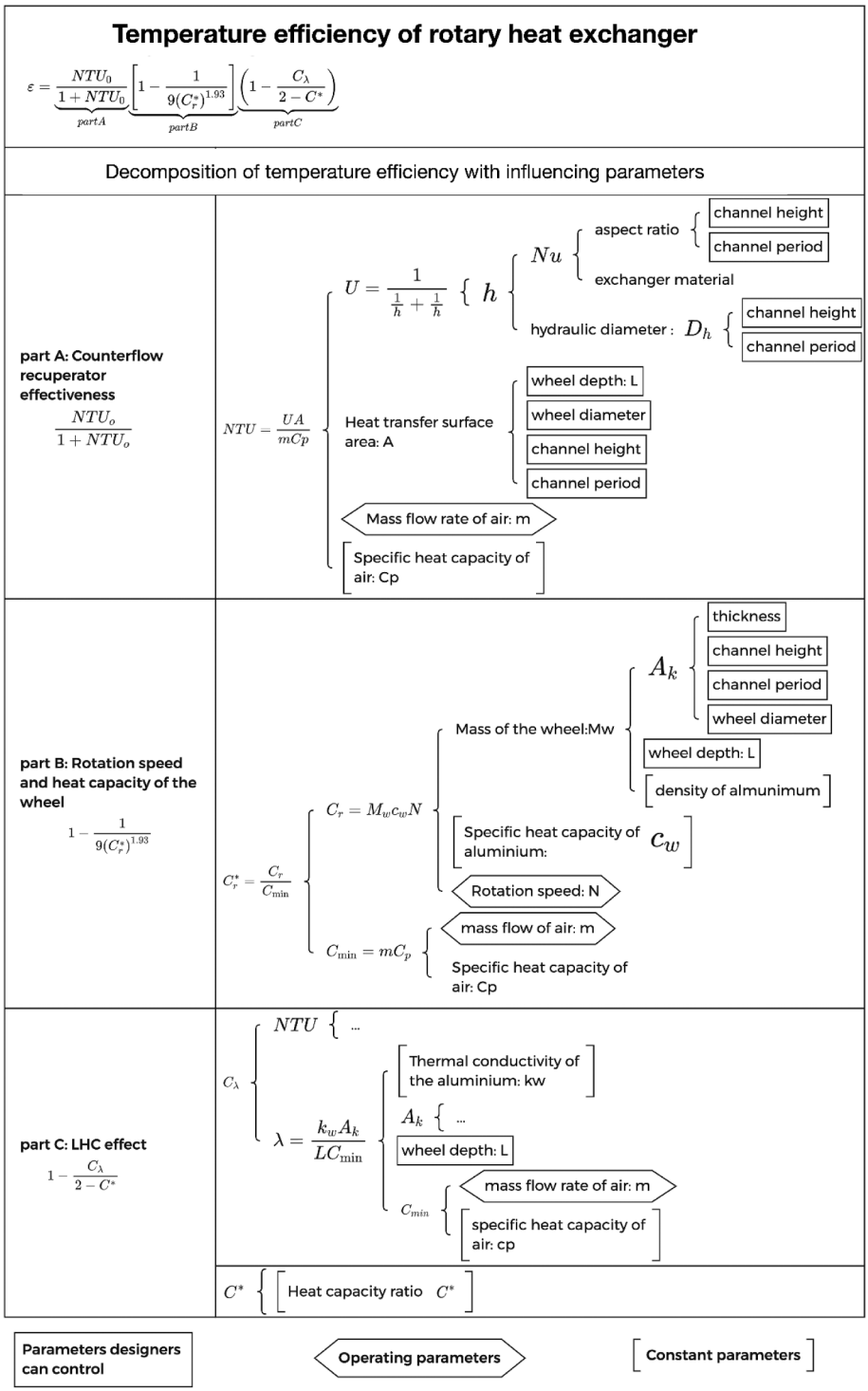

Fig. 3. Influential factors for the momentary temperature efficiency of rotary heat exchangers.

the temperature efficiency when frost prevention is on, which reduces the temperature efficiency.

In this study, the annual averaged temperature efficiency is defined as the arithmetic mean of the hourly efficiency when the exchanger is operating (i.e. when $\mathrm{Eff_i}$ is nonzero).

$$\mathrm{Eff}_{mean} = \frac{\int \mathrm{Eff}_{i,nonzero}}{N_{nonzero}} \tag{10}$$

The annual average efficiency is a function of the specifications of the rotary heat exchanger, the supply air temperature setpoint, the ventilation airflow rates and the frost protection, among other factors.

The core pressure drop through the rotary heat exchanger is calculated with Eq. (11):

$$\Delta p \approx \frac{4fLG^2}{2g_c D_h} \tag{11}$$

For a detailed determination of the input parameters and the pressure drop calculation, see [10,11].

2.2. Case building, ventilation and LHC effects in DCV

In this paper, we studied a virtual office building in Oslo, Norway. The building is assumed to comply with the Norwegian Building Regulation TEK17 [9]. The design occupancy density is 15 m^2/person, and the total building area changes according to the design occupant number. This study investigates the annual temperature efficiency and annual net energy savings for DCV with heat recovery.

Fig. 4 shows occupancy diversity factors on weekdays for office buildings from the Norwegian specification sN-NSPEK 3031 [25]. The number of occupants is reduced from hours 12 to 14 (i.e., from 12 to 2p.m.) on weekdays since some occupants leave the office for lunch or meetings. The building is assumed to be unoccupied on weekends.

The ventilation rates for DCV are assumed to respond ideally to the presence and number of occupants. The Norwegian building code requirements for ventilation airflow rates consist of two parts that must be summed: a) ventilating pollutants from occupants (26 m^3/h/person) and b) ventilating pollutants from building materials (2.5 m^3/h/m^2 when the room is in use and 0.7 m^3/h/m^2 otherwise) [9]. Hourly variations in ventilation rates and nominal occupants for the ventilation strategies and occupancy numbers are illustrated in Fig. 5.

The annual energy used for heating ventilation air is

$$Q_{ventilationheating} = \sum_{i=1}^{8760} \dot{m}_i c_p \left(t_{supply} - \left(Eff_i \left(t_{indoor} - t_{outdoor,i} \right) + t_{outdoor,i} \right) \right) \tau_i \tag{12}$$

where $\left(Eff_i \left(t_{indoor} - t_{outdoor,i} \right) + t_{outdoor,i} \right)$ is the air temperature leaving the heat exchanger on the supply side.

2.3. Global sensitivity analysis (GSA)

Sensitivity analysis (SA) measures the impact that changes in one or more input variables can induce in output variables [26]. SA is applied to estimate and rank the effects of different input parameters on the outputs of a model, which is known as factors prioritisation (FP). SA methods can be categorised as either local sensitivity analysis (LSA) or global sensitivity analysis (GSA). LSA generally entails changing one input at a time to test its effect on the output. In this approach, the sensitivity may be different if some other parameters are equal to different values; LSA does not take into account the effect of changing parameter values in the parameter space or simultaneous changes in the parameter set [27]. Another disadvantage of LSA is that it does not account for the impact of interactions between parameters [27].

GSA can overcome these limitations by providing the propagated uncertainty distribution in model usage or parameter estimation [28]. Among the various GSA methods, Sobol's method [29] is generally recognised as the most robust and efficient. This variance-based method decomposes the contribution of each input parameter to the variation of the output. Fig. 6 illustrates the variance-based GSA framework applied in this study. The principle of Sobol's method is that the model output's total unconditional variance can be quantified by decomposing it into the first-order, second-order and higher-order contribution terms. The first-order terms reflect the direct contribution of individual parameters. By evaluating the influence of an individual input on the output variation and its interaction with other inputs, Sobol's GSA reveals which input parameters significantly affect the output. Two different measures in Sobol's GSA are commonly used in combination: first-order sensitivity indices and total sensitivity indices. The former quantifies the main contributions of each single input parameter, while the latter quantifies the total effects consisting of first-order effects plus all interaction effects.

In this study, Sobol's GSA was used to quantify the contribution of each design parameter of rotary heat exchangers on the annual performance of heat recovery ventilation. The principle of Sobol's GSA is briefly introduced below.

Consider the following generic model:

$$Y = f(X_1, X_2 \cdots, X_k) \tag{13}$$

To quantify the importance of an input factor X_i on the variance of Y, consider that we can fix X_i at its 'true' value. The degree of the variance change of Y attributed to this assumption is the conditional variance. The variance of the conditional expectation, $V_{X_i}\left(E_{X_{\sim i}}(Y|X_i)\right)$, is considered as a summary measure of sensitivity. Then, the first-order sensitivity index of X_i on Y can be defined as Eq. (14) based on [27].

$$S_i = \frac{V_{X_i}\left(E_{X_{\sim i}}(Y|X_i)\right)}{V(Y)} \tag{14}$$

S_i is a number between 0 and 1. For purely additive models, the sum of first-order sensitivity indices of the input parameters is equal to 1 ($\sum_{i=1}^{d} S_i = 1$). For models that are not purely additive, in which interaction effects exist between input parameters, $\sum_{i=1}^{d} S_i < 1$. The difference $(1 - \sum_{i=1}^{d} S_i)$ indicates the strength of the interactions in the model.

Different parameters have different effects on the system's outcome. Higher values of S_i reflect more important input parameters X_i. $V_{X_i}\left(E_{X_{\sim i}}(Y|X_i)\right)$ is the expected variance reduction if X_i is fixed. Eq. (14) suggests that the influential factor is the one that causes a great reduction in variance when the given input factor is fixed to its true value (albeit unknown) within its range of uncertainty, while other input parameters vary within a defined interval [27]. The larger the reduction of output variance caused by fixing one factor, the larger its main effect and the greater its importance.

The total sensitivity indices S_{Ti} are another popular variance-based measure. They measure the total effect, including first and higher-order effects (interactions), of the input parameter X_i [30]. The total

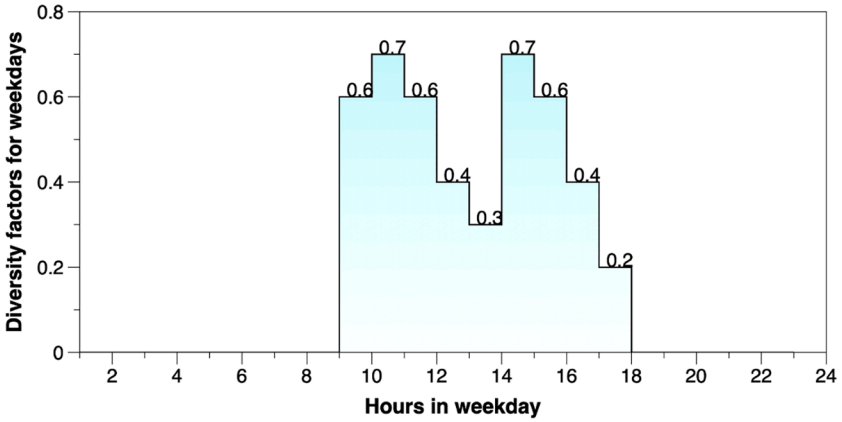

Fig. 4. Occupancy diversity factors on weekdays for office buildings.

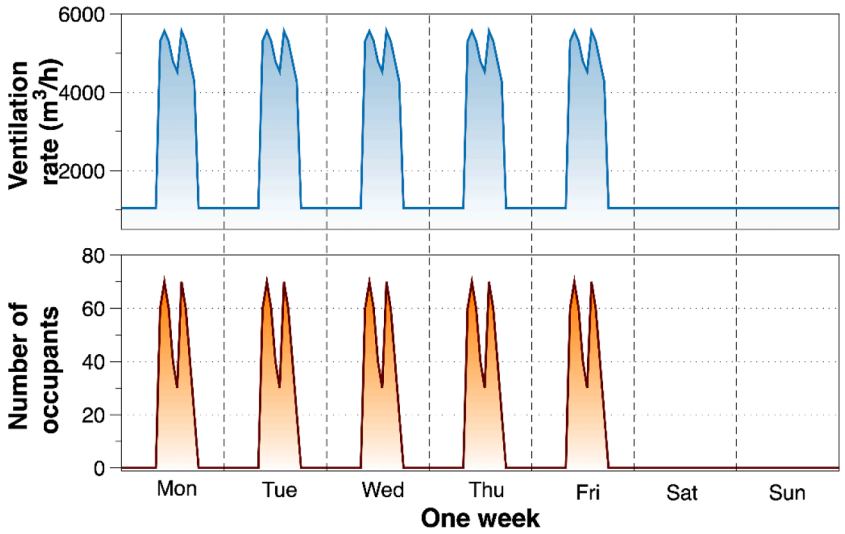

Fig. 5. Occupants and ventilation rates for DCV during a week used in this study.

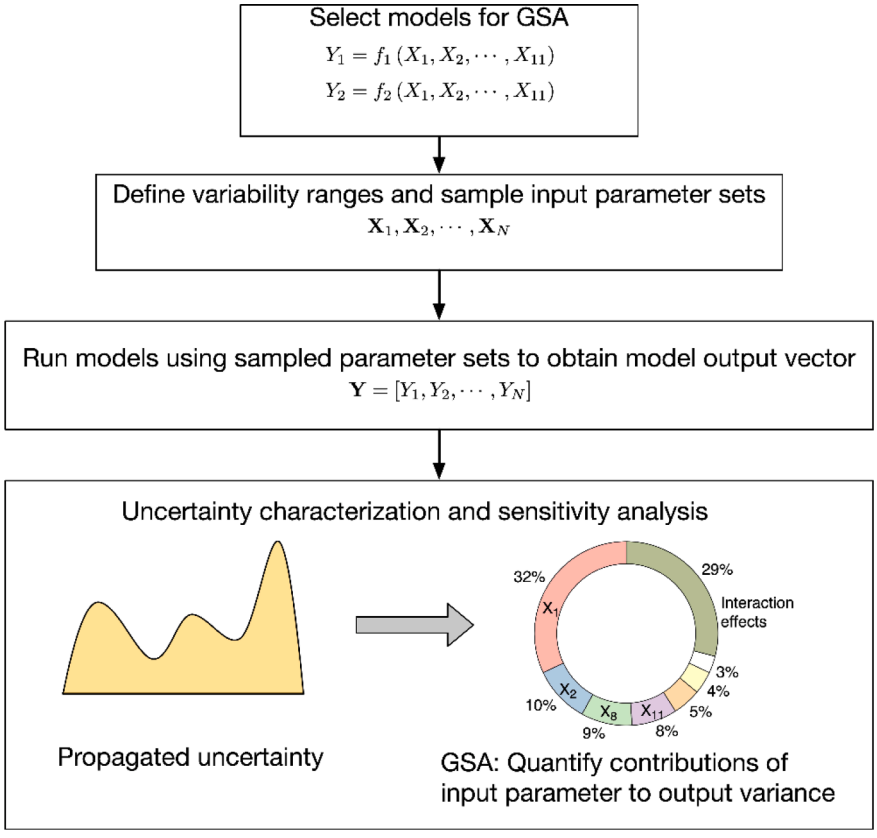

Fig. 6. Framework of the global sensitivity analysis used in this study.

sensitivity index is defined as follows:

$$S_{Ti} = \frac{E_{X_{\sim i}}(V_{X_i}(Y|X_{\sim i}))}{V(Y)} \tag{15}$$

where $X_{\sim i}$ is the vector $X_{\sim i} = (X_1, \cdots X_{i-1}, X_{i-1} \cdots X_d)^T$. By definition, S_{Ti} is equal to or greater than S_i. The difference between total sensitivity and first-order sensitivity, $(S_{Ti} - S_i)$, is a measure of the interaction effects of the input parameter X_i with any other input parameter [29].

One can identify the influential factors by ranking the parameter's main effects (first-order sensitivity). Furthermore, input parameters with a low first-order effect may have significant interaction effects with other parameters, which should also be considered important. For example, consider a simple model with two input parameters (X_1 and X_2). If both first-order sensitivity indices S_1 and S_2 for X_1 and X_2 are much smaller than S_{12}, this indicates that the interaction effects between X_1 and X_2 play an important role.

We explored the variability ranges of input parameters for first and total sensitivity indices using Sobol's quasi-random sequencing method [27]. For more detailed information about the GSA, see [27].

2.4. Optimisation of rotary heat exchanger

Fig. 7 shows the optimisation procedure to maximise the proposed annual net energy savings by using heat recovery. The constant inputs required to calculate the annual net energy savings are maximum occupant number, supply air temperature, indoor air temperature, frost protection temperature and fan efficiency. Six parameters were changed in the search for maximum annual net energy savings by heat recovery in DCV: the diameter of the rotary heat exchanger, the height of the corrugated channels, the period of the corrugated channels, the depth of the rotary heat exchanger, the thickness of the matrix, and the rotational speed. For a given ventilation rate profile, there is an optimal rotary heat exchanger design (the best combination of these six parameters) that yields the maximum total energy savings for a reference year. Table 2 displays the values of the constant inputs and the search ranges for the optimisation in this study.

The objective function considered here is the net energy savings for a reference year, which is calculated according to Eq. (16):

$$Q_{net} = \sum_{i=1}^{8760} \dot{m}_i c_p \left(t_{extract,i} - t_{outdoor,i}\right) \varepsilon_i \tau_i - \sum_{t=1}^{8760} \frac{\Delta P_i \dot{V}_i}{\eta_i} \tau_i \tag{16}$$

The first term on the right-hand side represents the energy recovered for a reference year using a rotary heat exchanger in a DCV. The second term represents the fan power used to overcome the pressure drop through the exchanger. Hourly temperature efficiency, ε_i, changes with the ventilation rates and with the modulations applied to achieve the temperature setpoints for supply air and frost protection. For the sake of simplicity, we assume a constant fan efficiency of 0.5.

In this study, the pattern-searching algorithm is applied in MATLAB to find the maximum net energy savings Q_{net} for the reference year using Eq. (16) as the objective function. Pattern-search methods proceed by performing a series of exploratory moves for the current iteration before declaring a new iteration and updating the associated information [31]. Pattern-search algorithms can look for a minimum based on an adaptive mesh, and they can be used on functions that are not continuous or differentiable since they do not require a gradient. Characterization and analysis of the pattern-search method are presented in [31]. Here, we take the negative value of the objective function to find the maximum. A constraint of the optimisation is that the aspect ratio of the channel must be within a range of $0 < \alpha < 1$.

3. Results and discussion

3.1. Validation of the mathematical model

The correlation for the temperature efficiency including the LHC effect is described in Eq. (1) and agrees with the results of the numerical solution using the finite difference discretisation method by Bahnke and Howard [13].

In this study, the empirical correlations of temperature efficiency and pressure drop presented in Section 2.1 were verified against experimental measurements. The measurements and sensors used in the test comply with the EN308 testing standard [22]. Fig. 8 shows the testing box for the rotary heat exchanger and its connections to the airflows. The experimental measurements of temperature efficiency and pressure drop through the developed heat wheels were conducted under the dry testing condition of the EN308 standard [22]. The outdoor air temperature was 5 °C, the extract air temperature was 25 °C, and the relative humidity of the extract air was lower than 30 %. Before and after the testing box, air static pressure was measured at the air ducts in the direction of the airflow. Measurements of the airflow rates were carried out with an uncertainty of ± 1.5 % using orifice plates with corner tapings, following ISO 5167 [32,33]. Temperatures were measured with Pt 100 sensors with an uncertainty of ± 0.1 °C. The static pressure measurements have a total uncertainty of 1 % of the measured values. The overall relative uncertainties of the measured efficiency and pressure drop were lower than ± 3 % and ± 5 %, respectively.

The specifications of the experimentally tested rotary heat exchanger are given in Table 1. We obtained acceptable agreement between calculated values from the empirical equations and experimental measurements for temperature efficiency and pressure drop over the different airflow rates (Fig. 9).

Based on Fig. 9(A), omitting LHC can lead to inaccurate temperature predictions and poor designs for rotary heat exchangers, especially for low airflow rates. Moreover, the trend of temperature efficiency in Fig. 9 (A) confirms that reducing airflow rates does not always increase temperature efficiency, as LHC has a greater impact on lower airflow rates. Hence, the LHC effect must be considered when designing highly efficient rotary heat exchangers. The measured pressure drops shown in Fig. 9(B) are slightly higher than the predicted values. This discrepancy could be attributed to the omission of entrance and exit pressure changes from the calculation.

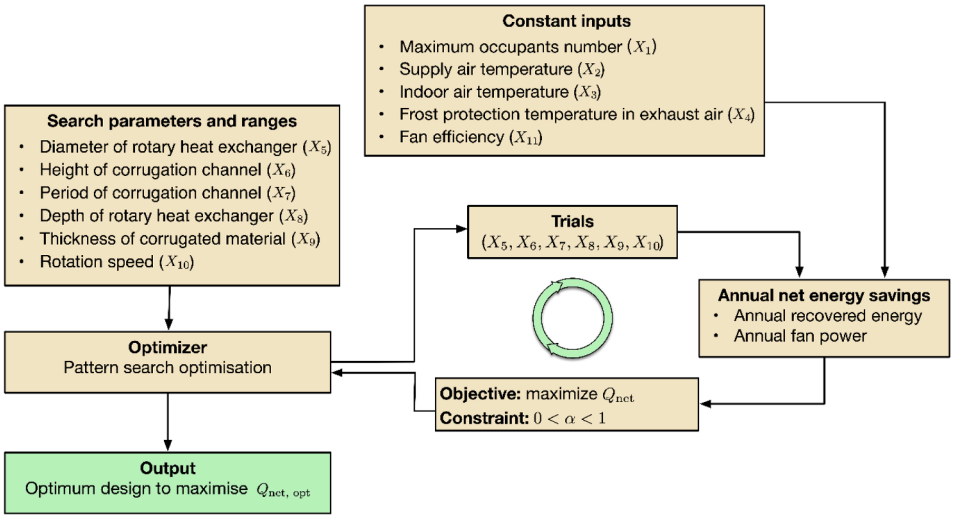

Fig. 7. Optimisation of rotary heat exchanger design to maximise annual net energy savings.

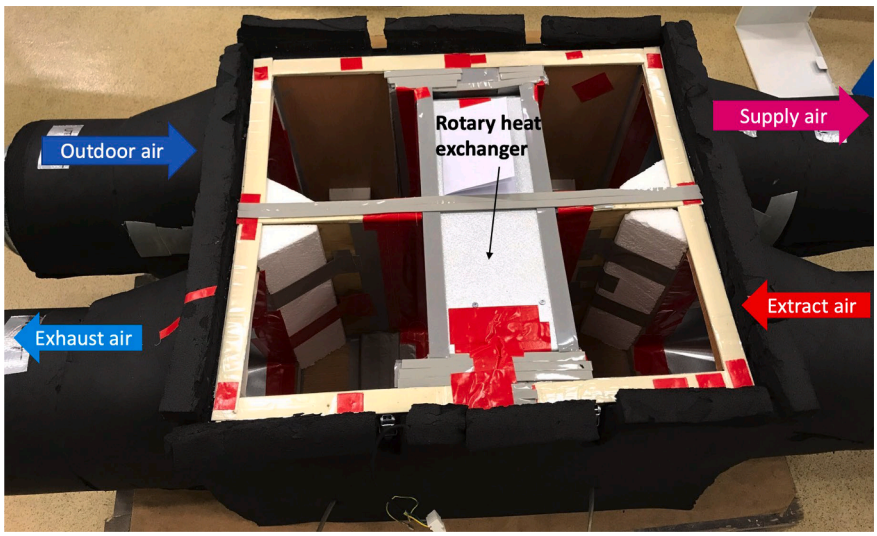

Fig. 8. Picture of the testing box including the tested rotary heat exchanger (adapted from [34]).

Table 1
Specifications of the tested rotary heat wheel.

Parameter	Value	Parameter	Value
Wheel depth	150 mm	Ventilation rate	50 m^3/h – 400 m^3/h
Wheel diameter	400 mm	Air density	1.2 kg/m^3
Matrix thickness	0.055 mm	Rotary speed	10 RPM
Matrix material	Aluminium $k = 205$ W/(m · K) $c_p = 900$ J/(kg · K)	Channel shape	Sinusoidal Channel height: 1.4 mm Channel period: 3.0 mm

3.2. GSA results for the annual temperature efficiency and annual net energy savings

The input parameters and their changing intervals are presented in Table 2. The variance-based Sobol's GSA method described in Section 2.3 is performed. The main influential factors on the annual performance of heat recovery through DCV are identified with the variance-based GSA.

The first-order and total sensitivity indices of the annual average temperature efficiency Eff_{mean} were computed using Eqs. (14) and. (15), with Eff_{mean} calculated according to Eq. (10). The sampling number for the changing range of the input parameters is 2,000 using Sobol's sequencing approach [28]. An input parameter is generally considered insignificant or irrelevant when its first-order sensitivity index is lower than 0.05. The results of the first-order and total sensitivity indices for the annual temperature efficiency are illustrated in Fig. 10. The figure shows that the impacts of the frost protection temperature (X_4), the thickness of the corrugation material (X_9), the rotational speed (X_{10}) and the specific fan power (X_{11}) are insignificant, as the first-order and total sensitivities of these four parameters are negligible. Therefore, changes in these four parameters within the variability ranges defined in this study have little impact on annual efficiency.

The pie chart at the top right of Fig. 10 shows the ranking of the first-order sensitivity of input parameters and their interaction effects. The supply air temperature setpoint (X_2) and the indoor (extract) air

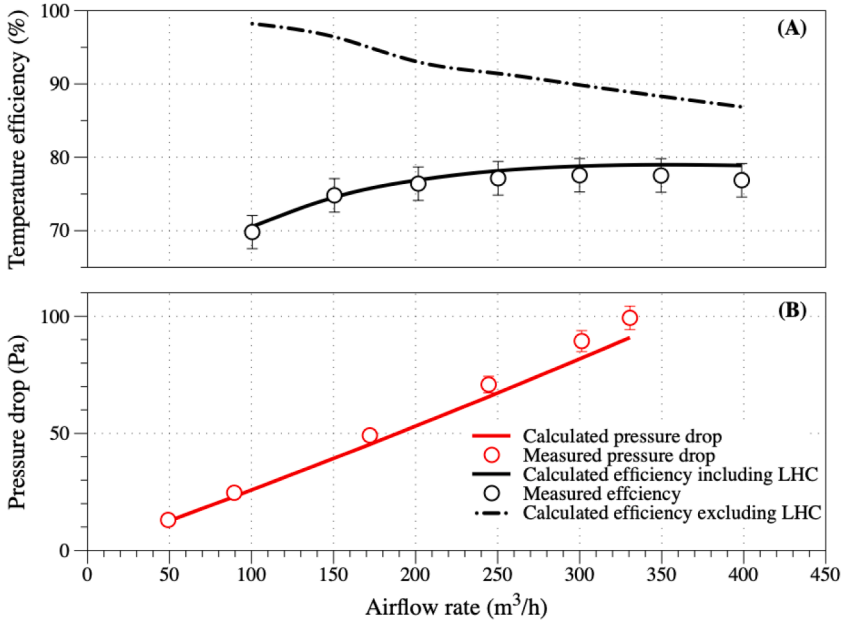

Fig. 9. Validation for (A) temperature efficiency and (B) pressure drop.

Table 2
GSA input parameters and changing ranges of interest.

ID	Input parameters [unit]	Range of interest [lower bound, upper bound]
X_1	Design occupant number [person]	[50, 100]
X_2	Supply air temperature [°C]	[16,20]
X_3	Indoor (extract) air temperature [°C]	[18,22]
X_4	Frost protection temperature of exhaust air [°C]	[-10, 0]
X_5	Diameter of rotary heat exchanger [mm]	[600, 1400]
X_6	Height of corrugated channel [mm]	[1,4]
X_7	Period of corrugated channel [mm]	[1,4]
X_8	Depth of rotary heat exchanger [mm]	[100, 300]
X_9	Thickness of corrugation material [mm]	[0.02, 0.08]
X_{10}	Rotational speed [RPM]	[6,15]
X_{11}	Specific fan power [kW/(m^3/s)]	[1.2, 2.5]

temperature (X_3) have the two most significant values of first-order sensitivity indices. Therefore, they have the most significant impact on annual average temperature efficiency as the main effect of changes in single input parameters. This can be attributed to the regulation of the supply and extract air temperatures to limit the operating temperature efficiency and avoid overheating the supply air. In this study, for GSA, the supply air temperature is set as a constant within a range of 16–20 °C. If the temperature of the air leaving the heat exchanger is higher than the supply air temperature setpoint, the exchanger's efficiency is reduced by reducing the rotational speed. This often occurs in the Oslo climate, as indicated by the GSA results. It should be noted that the setpoint of the supply air temperature (X_2) also has an impact on the energy use for space heating, which is not included in this study. The investigated system boundary in this study is limited to the air handling unit (AHU).

The sum of first-order sensitivity indices for all input parameters (0.52) is much lower than 1, which implies the presence of strong interaction effects between input parameters. These interaction effects are also indicated by the high values of the total sensitivity indices for the height and period of the corrugated channel (X_6 and X_7, respectively). As mentioned in Section 2.3, the first-order effects of X_6 and X_7 on annual efficiency are small. Nevertheless, these two parameters still play an important role and cannot be omitted, as they have relatively high interaction effects. In particular, they determine the aspect ratio of the channel and thus have a decisive impact on the heat transfer coefficient for a fully developed laminar flow; they also partially determine the total heat transfer area. In light of this finding, the aspect ratio of the sinusoidal channel should be carefully designed and constructed with the aim of achieving high annual temperature efficiency.

The first-order and total sensitivity indices for the annual net energy savings are shown in Fig. 11 with a sampling number of 2,200. These results reveal that the greatest effect is from the design occupant number (X_1) in comparison to all the other single input parameters (Fig. 11). This reflects the decisive role of occupant number in determining the ventilation airflow rates according to the ventilation regulation [25]. The supply air temperature setpoint (X_2), depth of rotary heat exchanger (X_8) and specific fan power (X_{11}) have similar impacts as single parameters on net annual energy savings.

The interaction effects between input parameters account for about one-third of the overall impact of all the parameters. As explained in Section 2.3, the difference between total sensitivity and first-order sensitivity indicates an input parameter's interaction effect with other parameters. Fig. 11 shows that the diameter of the rotary heat exchanger (X_5) has the highest interaction effect with other parameters on annual net energy savings. The impact of the frost protection temperature of exhaust air (X_4), the thickness of the corrugation material (X_9) and the rotation speed (X_{10}) can be neglected in the input range of interest.

It can be concluded that different factors should be prioritised to optimise annual efficiency or annual net energy savings. The four factors that have the most significant effects on annual energy savings are the maximum occupant number (X_1), the diameter of the rotary heat exchanger (X_5), the supply air temperature setpoint (X_2) and the depth of the rotary heat exchanger (X_8). The corresponding four most influential factors on annual efficiency are the height of the corrugated channel (X_6), the period of the corrugated channel (X_7), the supply air temperature (X_2) and the depth of the rotary heat exchanger (X_8). The impacts of the supply air temperature setpoint (X_2) and the depth of the wheel (X_8) are important for both annual temperature efficiency and annual net energy savings.

The most influential input parameters identified for annual efficiency and annual net energy savings are different. This may be because the effective recovered energy amount (denoted by Eq. (16)) considers the temperature difference between indoor and outdoor, ventilation rate profiles and fan power; in contrast, the annual efficiency (denoted by Eq. (10)) does not cover these factors.

3.3. *Optimisation of the rotary heat exchanger targeting the maximum net annual energy savings*

We optimised the parameters that designers can control for rotary heat exchangers in the defined range of interest to maximise the annual net energy savings (as denoted by the objective function Eq. (16)). The maximum iterations and function evaluations for optimisation are set to 20,000 and 15,000, respectively. The mesh tolerance and step tolerance are 1e-12. The input parameters, initial value and changing intervals are provided in Table 3.

This study aims to determine the parameters (X_5–X_{10}) that a designer

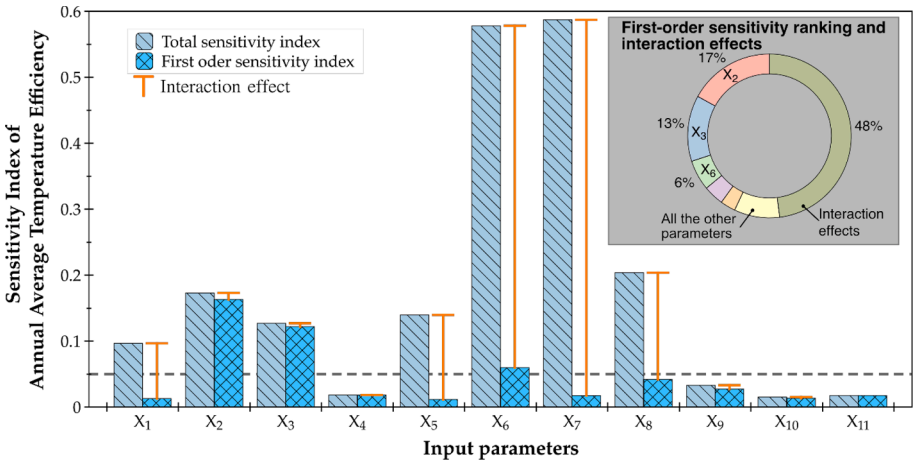

Fig. 10. First-order and total sensitivity index of input parameters for annual average temperature efficiency (X_1 – Design occupant number, X_2 – Supply air temperature, X_3 – Indoor (extract) air temperature, X_4 – Frost protection temperature of exhaust air, X_5 – Diameter of the rotary heat exchanger, X_6 – Height of the corrugated channel, X_7 – Period of the corrugated channel, X_8 – Depth of rotary heat exchanger, X_9 – Thickness of corrugation material, X_{10} – Rotational speed, X_{11} – Specific fan power).

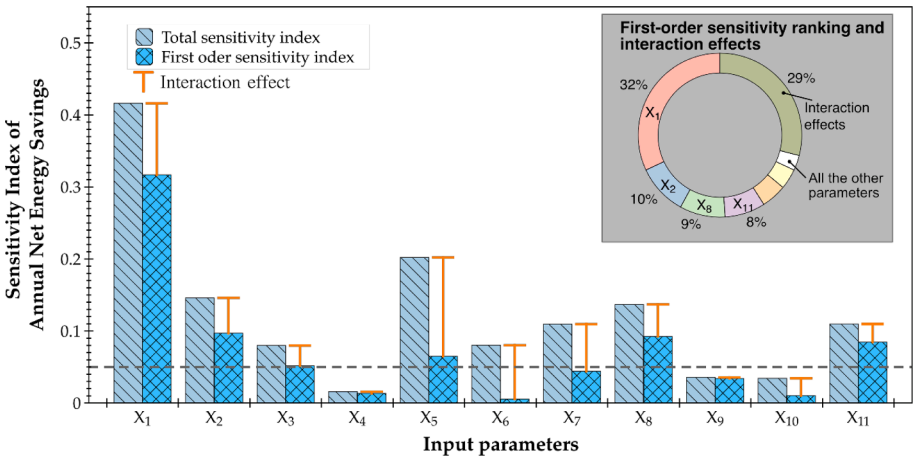

Fig. 11. First-order and total sensitivity index of input parameters for annual net energy savings (X_1 – Design occupant number, X_2 – Supply air temperature, X_3 – Indoor (extract) air temperature, X_4 – Frost protection temperature of exhaust air, X_5 – Diameter of rotary heat exchanger, X_6 – Height of corrugated channel, X_7 – Period of corrugated channel, X_8 – Depth of rotary heat exchanger, X_9 – Thickness of corrugation material, X_{10} – Rotational speed, X_{11} – Specific fan power).

can control on a rotary heat exchanger to obtain maximum net annual energy savings. The maximum occupant number (X_1), supply air temperature (X_2), indoor air temperature (X_3), frost protection temperature (X_4) and fan efficiency (X'_{11}) have been fixed as constant input parameters. The optimisation of annual net energy savings is complicated by the fact that some factors in the objective function Eq. (16) counteract each other. For instance, increasing the depth of the rotary heat exchanger enlarges the heat transfer area and results in higher heat recovery rates. However, increasing the exchanger depth also increases the pressure drop through the exchanger, which increases the fan power. As a result, it is necessary to seek an optimal combination of the parameters that maximises the annual net energy savings considering both recovered energy and extra fan power consumption by using a heat exchanger. It should be pointed out that we did not consider the pressure drop of the rest of the ventilation system, as it is case-dependent for different ventilation ductwork sizes, layouts, filters and other ventilation components. Only the pressure drop through the heat recovery is included in the optimisation (Table 3).

The maximum annual net energy was investigated for different design occupant numbers (50, 100 and 150). The optimisation process for these different occupant numbers is illustrated in Fig. 12. All the optimisations substantially improve the annual net energy savings. For instance, at a design occupant number of 50, the annual recovered energy can be increased by up to 48 % by optimising the design of the rotary heat exchanger. The relative increase in net energy savings grows as the design occupant number decreases from 150 to 50. Nevertheless, optimisation recovers more energy for large buildings (absolute increase) than small office buildings. It should be noted that optimisation for different sizes of buildings has been conducted with the same initial input parameters of the rotary heat exchanger. This is not a realistic representation of the design process. However, the aim of the study is to demonstrate that the pattern-search optimisation technique is a viable method that can be applied to optimise the design of rotary heat exchangers aiming to maximise annual net energy savings.

Table 4 shows that the optimum diameter of the exchanger increases with the design occupant number. The maximum annual net energy savings are achieved with a thin matrix, which reduces the LHC and the heat capacity of the rotary heat exchangers. Within the study's search ranges, the maximum rotational speed of 15 RPM always contributes to maximising the annual net energy savings. However, higher rotational speeds may result in higher levels of cross-contamination due to higher carryover rates. 300 mm is set as the upper bound of the depth of the rotary heat exchanger mainly due to the volume of the AHU.

It should be noted that the optimisation was performed under constant supply, extract air and frost protection temperatures to ease the optimisation (Table 3). In practice, these temperatures depend strongly on the design of the building automation system, commissioning and maintenance. As Fig. 11 shows, the contribution of extract air and frost air temperature to the annual energy savings is negligible. As a result, the influence of fluctuations in these temperatures can be ignored. Using the optimised heat wheels for different design occupant numbers, the supply air temperature, which is in the range of 16–20 °C, gives a maximum relative difference of 7.8 % for the optimised annual energy savings.

Table 3
Input parameters, initial values and their changing intervals for optimisation.

ID	Input parameters [unit]	Initial value	Search range [lower bound, upper bound]
X_1	Design occupant number [person]	50	Constants (50, 100, 150)
X_2	Supply air temperature [°C]	18	Constant
X_3	Indoor air temperature [°C]	21	Constant
X_4	Frost protection temperature of exhaust air [°C]	−5	Constant
X_5	Diameter of rotary heat exchanger [mm]	1,500	[1,000, 2,500]
X_6	Height of corrugation channel [mm]	2.0	[1,4]
X_7	Period of corrugation channel [mm]	3.0	[1,4]
X_8	Depth of rotary heat exchanger [mm]	100	[50, 300]
X_9	Thickness of corrugated material [mm]	0.05	[0.02, 0.1]
X_{10}	Rotation speed [RPM]	8	[6,15]
X'_{11}	Fan efficiency	0.5	Constant

3.4. Limitations of this study

1. This study only investigated a single Norwegian city, Oslo. Oslo weather data was chosen to be representative of cold climates. More regions in cold climates could be studied and compared with the proposed methods.
2. In this study, only the occupancy profile in the design standard is used to prescribe the ventilation rates. The paper focuses on demonstrating the use of GSA and optimisation to explore the effect of different input parameters and increase annual net energy recovery. However, measured ventilation data can also be used to obtain more realistic ventilation rate profiles for further study.

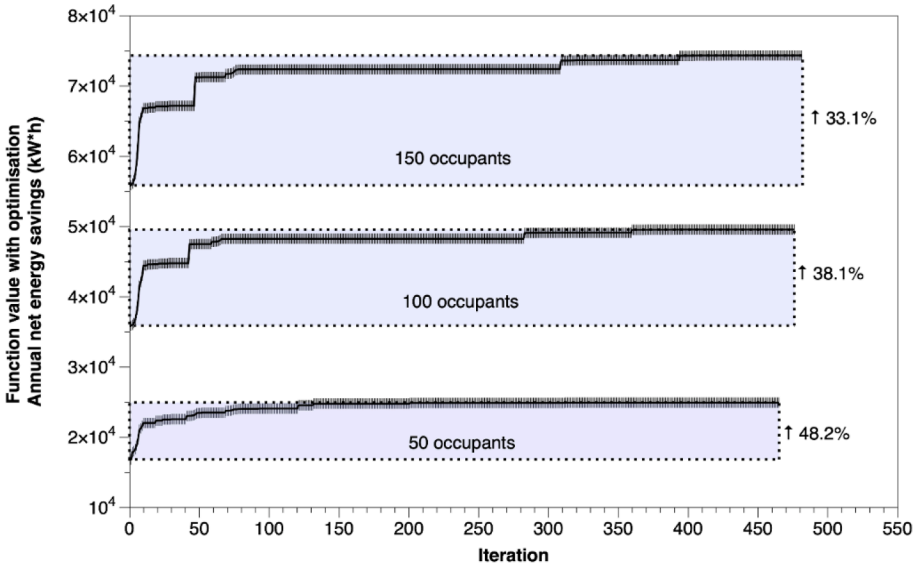

Fig. 12. The optimisation process for rotary heat exchangers to maximise annual net energy savings in DCV for different design occupant numbers.

Table 4
Optimal designs of rotary heat exchangers for different design occupant numbers.

Design occupant number	Diameter of rotary heat exchanger [mm]	Height of corrugated channel [mm]	Period of corrugated channel [mm]	Depth of rotary heat exchanger [mm]	Thickness of matrix [mm]	Rotational speed [RPM]
50	1211	2.8	2.2	300	0.026	15
100	1385	2.3	2.2	300	0.050	15
150	1835	2.3	2.2	300	0.034	15

4. Conclusions

This paper decomposes the empirical determination of the temperature efficiency for rotary heat exchangers in ventilation systems. The LHC effect, which is often overlooked but results in efficiency loss at low airflow rates, is taken into account in variance-based GSA and optimisation of rotary heat exchangers. We obtained a good agreement between the theoretical calculations and experiential measurements for temperature efficiency and pressure drop. The distinct effects of these design input parameters and the effects among their interactions on annual temperature efficiency and annual net energy savings have been quantified with the variance-based GSA method. The optimal designs of the rotary heat exchangers for annual net energy savings were implemented through pattern-search optimisation. The energy used for heating ventilation air was revealed in DCV, taking into account the LHC effect in rotary heat exchangers. The main findings are as follows:

1. The GSA results for annual temperature efficiency show that the supply air temperature setpoint and indoor air temperature, as single input parameters, have the most significant impacts when the rotary heat exchanger is used in DCV. Despite low first-order effects of the height and period of the corrugated channel on annual efficiency, the interaction effects between these two parameters play an important role.
2. The amount of annual net energy savings is strongly influenced by the design occupant number (building size) and the resulting ventilation rate profiles in a DCV. Parameters and their interactions, such as the frost protection temperature of exhaust air, the thickness of corrugated material and rotation speed, have negligible effects on annual net energy savings. Suppose the design occupant number is fixed for a specific building. The energy savings are mainly influenced by the parameters including supply air temperature setpoint, depth and diameter of the rotary heat exchanger and specific fan power.
3. The optimisation of the heat wheel design parameters using the pattern-search approach can significantly increase energy savings. For an office building equipped with DCV and a design occupant number of 50, the annual net energy savings can increase by 48 % with the optimal design compared to the baseline rotary heat exchanger. Accordingly, accurate and practical information about a building's occupants and usage will help to design optimal rotary heat exchangers that achieve the maximum amount of energy savings.
4. Longitudinal heat conduction in the metallic matrix degrades the temperature efficiency, causing the heat exchanger to recover less energy. The inefficiency effect is more evident for lower airflow rates and deeper exchangers. Therefore, considering both the LHC effect and the high pressure drop penalty, designs with deep rotary heat exchangers should be avoided.

Declaration of Competing Interest

The authors declare that they have no known competing financial interests or personal relationships that could have appeared to influence the work reported in this paper.

Data availability

No data was used for the research described in the article.

Acknowledgements

This paper has been written within the Research Centre on Zero Emission Neighbourhoods in Smart Cities (FME ZEN). The authors gratefully acknowledge the support from the ZEN partners and the

Research Council of Norway (project number 257660).

References

[1] Chenari B, Dias Carrilho J, Gameiro Da Silva M. Towards sustainable, energy-efficient and healthy ventilation strategies in buildings: A review. Renew Sustain Energy Rev 2016;59:1426–47.

[2] Harish VSKV, Kumar A. A review on modeling and simulation of building energy systems. Renew Sustain Energy Rev 2016;56:1272–92. https://doi.org/10.1016/j.rser.2015.12.040.

[3] Yang L, Yan H, Lam JC. Thermal comfort and building energy consumption implications - A review. Appl Energy 2014;115:164–73.

[4] Jing G, Cai W, Zhang X, Cui C, Liu H, Wang C. An energy-saving control strategy for multi-zone demand controlled ventilation system with data-driven model and air balancing control. Energy 2020;199:117328. https://doi.org/10.1016/J.ENERGY.2020.117328.

[5] Cuce PM, Riffat S. A comprehensive review of heat recovery systems for building applications. Renew Sustain Energy Rev 2015;47:665–82. https://doi.org/10.1016/j.rser.2015.03.087.

[6] Nourozi B, Wang Q, Ploskić A. Energy and defrosting contributions of preheating cold supply air in buildings with balanced ventilation. Appl Therm Eng 2019;146:180–9. https://doi.org/10.1016/J.APPLTHERMALENG.2018.09.118.

[7] Bai HY, Liu P, Justo Alonso M, Mathisen HM. A review of heat recovery technologies and their frost control for residential building ventilation in cold climate regions. Renew Sustain Energy Rev 2022;162:112417. https://doi.org/10.1016/J.RSER.2022.112417.

[8] Justo Alonso M, Liu P, Mathisen HM, Ge G, Simonson C. Review of heat/energy recovery exchangers for use in ZEBs in cold climate countries. Build Environ 2015;84:228–37. https://doi.org/10.1016/j.buildenv.2014.11.014.

[9] TEK17 (2017) Veiledning om tekniske krav til byggverk, Byggteknisk forskrift (TEK17) med veiledning. Ikrafttredelse 1. juli 2017, Direktoratet for byggkvalitet.

[10] Liu P, Justo Alonso M, Mathisen HM. Heat recovery ventilation design limitations due to LHC for different ventilation strategies in ZEB. Build Environ 2022;224:109542. https://doi.org/10.1016/j.buildenv.2022.109542.

[11] Shah RK, Sekulic DP. Fundamentals of Heat Exchanger Design. John Wiley & Sons; 2003.

[12] Liu P, Mathisen HM, Alonso MJ. Theoretical Prediction of Longitudinal Heat Conduction Effects on the Efficiency of the Heat Wheel used for Ventilation in Powerhouse Building "kjørbo" in Norway. Energy Procedia 2017;105:4949–54.

[13] Bahnke GD, Howard CP. The Effect of Longitudinal Heat Conduction on Periodic-Flow Heat Exchanger Performance. J Eng Power 1964;86:105. https://doi.org/10.1115/1.3677551.

[14] Schibuola L, Scarpa M, Tambani C. CO2 based ventilation control in energy retrofit: An experimental assessment. Energy 2018;143:606–14.

[15] Merema B, Delwati M, Sourbron M, Breesch H. Demand controlled ventilation (DCV) in school and office buildings: Lessons learnt from case studies. Energy Build 2018;172:349–60. https://doi.org/10.1016/J.ENBUILD.2018.04.065.

[16] Xu X, Wang S, Sun Z, Xiao Fu. A model-based optimal ventilation control strategy of multi-zone VAV air-conditioning systems. Appl Therm Eng 2009;29(1):91–104.

[17] Liu P, Justo Alonso M, Mathisen HM, Halfvardsson A. Development and optimization of highly efficient heat recoveries for low carbon residential buildings. Energy Build 2022;268:112236. https://doi.org/10.1016/J.ENBUILD.2022.112236.

[18] Liu P, Justo Alonso M, Mathisen HM, Simonson C. Performance of a quasi-counter-flow air-to-air membrane energy exchanger in cold climates. Energy Build 2016;119:129–42. https://doi.org/10.1016/j.enbuild.2016.03.010.

[19] Rao RV, Saroj A, Ocloń P, Taler J. Design Optimization of Heat Exchangers with Advanced Optimization Techniques: A Review. Arch Comput Methods Eng 2020;27:517–48. https://doi.org/10.1007/S11831-019-09318-Y.

[20] De Antonellis S, Intini M, Joppolo C, Leone C. Design Optimization of Heat Wheels for Energy Recovery in HVAC Systems. Energies 2014;7(11):7348–67.

[21] Rafati Nasr M, Fauchoux M, Besant RW, Simonson CJ. A review of frosting in air-to-air energy exchangers. Renew Sustain Energy Rev 2014;30:538–54. https://doi.org/10.1016/j.rser.2013.10.038.

[22] BS EN 308:1997 - Heat exchangers. Test procedures for establishing the performance of air to air and flue gases heat recovery devices n.d.

[23] EN 13141-1:2019 - Ventilation for buildings - Performance testing of components/products for n.d.

[24] Roulet C-A, Heidt FD, Foradini F, Pibiri M-C. Real heat recovery with air handling units. Energy Build 2001;33(5):495–502.

[25] SN-NSPEK 3031:2020 Energy performance of buildings — Calculation of energy needs and energy supply (only in Norwegian).

[26] Pichery C. Sensitivity Analysis. Encycl Toxicol Third Ed 2014:236–7. https://doi.org/10.1016/B978-0-12-386454-3.00431-0.

[27] Saltelli A, Ratto M, Andres T, Campolongo F, Cariboni J, Gatelli D, Saisana M, Tarantola S, editors. Global Sensitivity Analysis. The Primer. Wiley; 2007.

[28] Bassaganya-Riera J. Computational Immunology: Models and Tools. Comput Immunol Models Tools 2015:1–200. https://doi.org/10.1016/C2015-0-00090-9.

[29] Sobol IM. Global sensitivity indices for nonlinear mathematical models and their Monte Carlo estimates. Math Comput Simul 2001;55:271–80. https://doi.org/10.1016/S0378-4754(00)00270-6.

[30] Saltelli A, Annoni P, Azzini I, Campolongo F, Ratto M, Tarantola S. Variance based sensitivity analysis of model output. Design and estimator for the total sensitivity index. Comput Phys Commun 2010;181:259–70. https://doi.org/10.1016/J.CPC.2009.09.018.

[31] Torczon V. On the Convergence of Pattern Search Algorithms. SIAM J Optim 1997;7(1):1–25.

[32] ISO 5167-1:2003. Measurement of fluid flow by means of pressure differential devices - Part 1: Orifice plates, nozzles and Venturi tubes inserted in circular cross-section conduits running full, International Standards Organization, Geneva, Switzerland.; 2003.

[33] ISO 5167-2:2003. Measurement of fluid flow by means of pressure differential devices inserted in circular cross-section conduits running full – Part 2: Orifice plates n.d. International Standards Organization, Geneva, Switzerland.; 2003.

[34] Liu P, Justo Alonso M, Mathisen HM, Halfvardsson A. The use of machine learning to determine moisture recovery in a heat wheel and its impact on indoor moisture. Build Environ 2022;215:108971. https://doi.org/10.1016/J.BUILDENV.2022.108971.